Excitation energy transfer and charge exchange during collisions of $N^+(^1S)$ and $N^+(^5S)$ with N_2

K. B. McAfee, Jr., C. R. Szmanda, and R. S. Hozack
AT&T Bell Laboratories, Murray Hill, New Jersey 07974
(Received 1 December 1986)

Measurements of charge exchange between N^+ and N_2 are reported for low product-ion energies and nearly zero center-of-mass scattering angles. The principal scattering is attributed to $N^+(^1S)$ with major contributions from the ^5S state. Fine structure corresponding to the transfer of excitation energy between the incident ion and the vibrational states of the target species has been measured. The results are interpreted in terms of a model involving the compensation of deflections produced by attractive and repulsive potentials at distances larger than the potential minimum of the N^+-N_2 system. No "selection rule" for vibrational energy transfer such as has been observed for N_2^+ on N_2 is found.

INTRODUCTION

The reactions of ground-state and metastable N^+ (^3P and ^1D) with molecular nitrogen at relatively low impact energies have been extensively studied.[1-7(a)] Information concerning the atomic N^+ ion is important in astrophysics because the very long lifetime of the metastable states which give rise to nebular lines permit their detection[8-10] at low interstellar densities. N^+ is a principal component of the earth's upper atmosphere[11,12] and therefore plays an important role in determining the propagation of electromagnetic signals in the D and E layers of the ionosphere. N^+ is also important in the chemistry of the initial stages of atmospheric ionization during meteor entry.[13] In addition, collisions between N^+ and nitrogen can represent an important energy-loss mechanism in lasers.

For these reasons as well as interest in the basic properties of the system, studies of the mobility of N^+ is its parent gas have been intensively pursued by a number of investigators.[14,15] Increased interest in the system has led Moore,[16] Rutherford,[17] Moran,[6,7(a)] and others to make measurements involving ground and excited states of N^+ and these researchers have greatly furthered knowledge concerning the complex processes in the nitrogen system. Despite the large number of studies conducted up to the present, atmospheric deionization processes, for example, are still not thoroughly understood and this study has been conducted to determine the relative importance of some of the reactions of the metastable states of N^+.

A principal difficulty in experiments seeking to define the N^+ system has been the occurrence of N_2^{2+} molecular ions which are produced in sources of N^+ and which are not discriminated from N^+ by the conventional momentum analysis technique. A recent analysis of the occurrence of effects of N_2^{2+} in crossed-beam experiments has been carried out by Schulz[7(b)] which demonstrates that in N^+ on Ar collisions N_2^+ can be important in producing several percent of the scattering intensity. The effects reported are, however, at higher product-ion energies than those reported in this work. Another difficulty in the N^+-N_2 system is the complex array of at least three atomic metastable projectile-ion electronic states as well as the two atomic and three molecular product-ion and neutral electronic states which need to be considered. However, the presence of this large number of electronic states also has virtue in that it allows and extensive study of the effect of the energy defect upon the cross section of the various reactions which take place.

This paper reports some new results concerning the importance of ^1S and ^5S states in very-low center-of-mass deflection charge-exchange experiments. Because of the high resolution of the experiment with respect to the product-ion energy and differential scattering angle, it is possible to draw a distinction between the expected deflections of the various reactant states. Also, we are able to determine how the positive-energy defect of the reaction can be converted efficiently into a maximum of five or six vibrational quanta of the N_2^+ product ion.

EXPERIMENT

The cross-beam apparatus used in this study has been described briefly in Ref. 18. It basically consists of well-defined atomic ion and molecular beams whose energy can be carefully determined. The experiment differs from most previous techniques in that the energy of the slow product ion and its angle of deflection are measured rather than the small deflection of the fast projectile ion. The angle of deflection in laboratory coordinates is measured in the plane of the two velocity vectors from $\theta_{lab} = -30°$ to $+90°$, where the angle of deflection, θ_{lab}, of the slow product ion is considered positive if the production-ion velocity has a component in the direction velocity of the projectile ion. Figure 1 shows the relationship of the various velocities and angles.

Thus the charged products of all endothermic reactions are deflected into the positive region of laboratory-angle space while most exothermic reactions of low product-ion energy result in deflections into negative an-

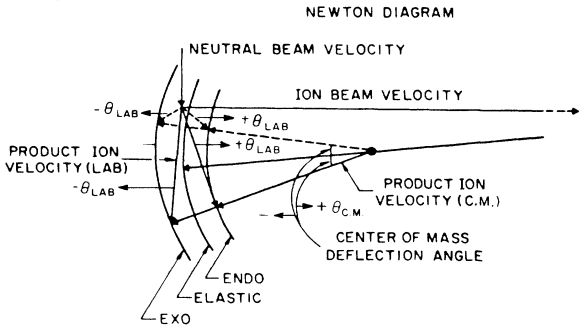

FIG. 1. Schematic Newton diagram for a 90° collision between a fast projectile ion and a neutral target. The resultant vectors show the velocity of the target species after collisions. The dotted vector shows a collision totally equivalent in the c.m. system, but which is observed at a different and usually overlapping the laboratory deflection angle and energy position. Arcs indicate loci of velocity vectors for exothermic, elastic, and endothermic collisions.

gles. High resolution of the laboratory deflection angle at about 1.4° and 0.04 eV [full width at half maximum (FWHM)] can be obtained in our experiments by employing a molecular beam from a fully expanded jet which has a very narrow velocity distribution and a low angle of dispersion.

Several methods of calibration of the energy measured by the analyzer have been employed. These include, for comparison, ionization of the neutral beam by electron impact and a pulsed time-of-flight determination of the velocity of the ions. The energy of the fully expanded neutral beam of N_2 is about 0.071 eV.

Most details of our apparatus have been previously described. However, we have fully automated the scanning and detection systems and have developed a technique for displaying the results in the form of topographical intensity contours in the product-ion-energy laboratory-deflection-angle plane.[19] It is important to realize that we measure the charge-transfer process, not the direct process which is measured in most experiments elsewhere.

RESULTS AND DISCUSSION

Table I shows the possible charge-exchange reactions in the N^+-N_2 system, typified by Eq. (1),

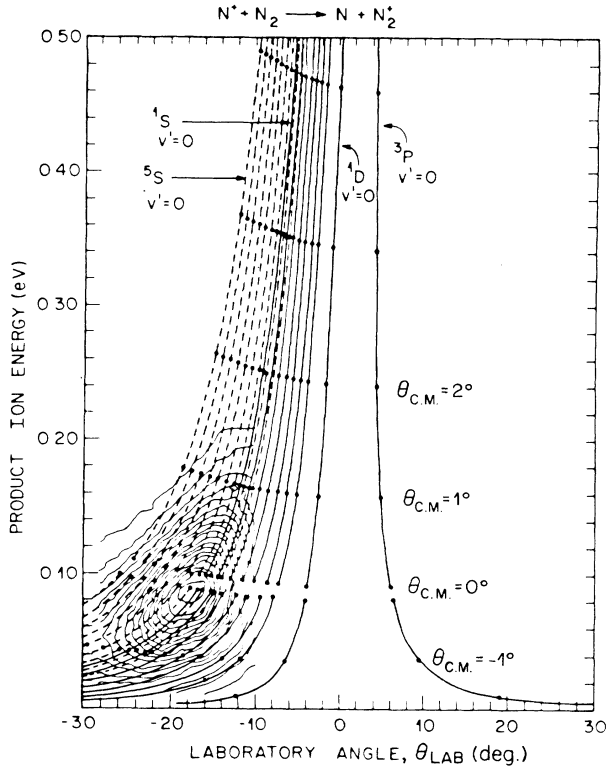

FIG. 2. Differential scattering contours for the reaction $N^+ + N_2 \rightarrow N + N_2^+$. The isointensity scattering contours are centered at $-17°$. Each scattering contour line differs from the adjacent contour lines by a constant value of 5%. Superimposed on the contours are axes which represent the center-of-mass deflection in degrees projected into the laboratory reference frame. The marks on these curves represent 1° c.m. deflection. The dotted curves represent those reactions which come from the ^5S state nitrogen while the solid curves represent similar reactions with the ^1S state. Within a bundle of curves, each curve represents a single product-ion vibrational state. Only the center-of-mass deflection axes corresponding to the ^1D and ^3P states of N^+ which produce products in $v'=0$ are also shown.

$$N^+(^1S)+N_2(^1\Sigma_g^+)\rightarrow N(^4S)+N_2^+(^2\Sigma_g^+)\,. \qquad (1)$$

The number within the last three columns represent the energy defects for processes involving pairs of projectile ions and product ions. Only the first three of the five

TABLE I. Recombination energies (Ref. 20) and energy defects (Refs. 21 and 22) in eV for $N^+ + N_2 \rightarrow N + N_2^+$ charge-transfer processes.

Projectile ion	Electron recombination energy	Reaction energy (Energy defect) $N_2^+ X(^2\Sigma_g^+)$		$N_2^+ A(^2\Pi_u)$		$N_2^+ B(^2\Sigma_u^+)$	
		$N(^2D)$	$N(^4S)$	$N(^2D)$	$N(^4S)$	$N(^2D)$	$N(^4S)$
$N^+(^3P)$	14.534		−1.047		−2.185		−4.204
$N^+(^1D)$	16.433	−1.532	0.852	−2.669	−0.285	−2.305	
$N^+(^1S)$	18.587	0.622	3.006	−0.515	1.869	−2.535	−0.150
$N^+(^5S)$	20.287		4.706		3.569		1.550

well-characterized N_2^+ states are listed in the table. The first column shows the four principal atomic ions which we believe are produced in easily measurable quantities in electron single-impact sources at about 100 eV impact energy. The last three columns are further divided so that we consider reactions in which the fast neutral product species is in the ground ^4S or ^2D states of the nitrogen atom. The energy defects shown are those which we believe would produce deflections within the portion of energy–laboratory-angle space which is explored in this work.

Table I is to be compared with the data shown in Fig. 2. It displays the nearly circular contours of equal scattering intensity of N_2^+ ions resulting from collisions with relative impact energy of 132 eV. Superimposed on the plot are center-of-mass deflection axes which correspond to a constant reaction energy defect.

The points on these axes indicate the center-of-mass angle deflection in one degree increments. The solid curves represent $N^+(^1S)$, $N^+(^1D)$, and $N^+(^3P)$, respectively. Each line within the bundle of ^1S and ^5S curves indicates the vibrational state of the product N_2^+ molecule. The dotted lines indicate the expected set of deflections corresponding to the ^5S state of the nitrogen ion. The maximum of the contours occurs at the laboratory deflection angle of about $-17°$ and a measured laboratory energy of about 0.09 eV. The product-ion energy measured corresponds to nearly zero center-of-mass angle deflection and it indicates that the speed of the target molecular-beam molecules is not significantly altered by the charge-exchange process.

Careful examination of the contours of Fig. 2 indicates significant broadening of the scattering pattern to the negative side of the center at a laboratory deflection angle of 17°, while the contours toward the positive side of the center are relatively more abrupt. It should also be noted that the shape of the intensity contour lines tend to approximate the shape of the loci of possible deflections determined from the Newtonian calculations which have been superimposed on the scattering contours. Figure 2 only represents scattering occurring with very low product-ion energy and therefore is not intended to represent all the scattering which would be included in a total charge-exchange measurement.

Figure 3 represents the scattering intensity scan as a function of product-ion energy taken at a constant laboratory deflection angle of $-17°$ which bisects the peak of the scattering contours. The data shown displays the particle count, normalized to the measured projectile ion beam current, versus the measured product-ion energy. For the curve shown, it will again be observed that the shape is not symmetrical. As the measured energy increases (cf. Fig. 2), it is seen that product-ion energies which are greater than 0.09 eV fall within expected energies from the ^5S state as predicted from the Newtonian calculation.

The curve drawn throughout the points of Fig. 3 has been produced by means of a fifth-order spline fitting program.[23] The use of a fifth-order spline in interpreting our data enables a refinement in the determination of fine structure in that the behavior of both first and

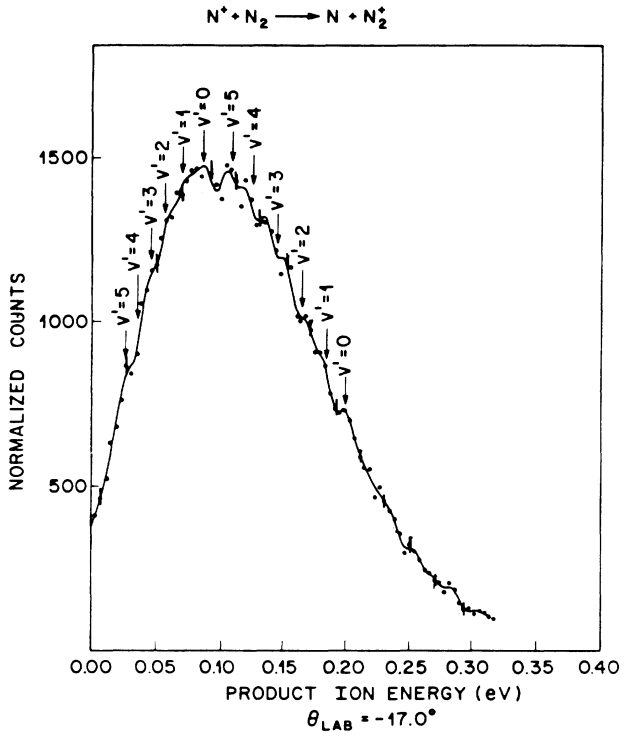

FIG. 3. This figure represents a scan in energy at a constant laboratory angle of $-17°$. The various scattering maxima correspond well to the expected position of the peak scattering of the vibrational states of the product molecular ion. The two electronic states of the projectile N^+ are ^5S and ^1S. The solid curve was calculated from a fifth-order spline function.[23].

second derivatives can be employed in measuring the peak position. The position of the arrows shown in Fig. 3 is compared with the value obtained from the second derivative of the curve produced by the fit of the data by least squares to the fifth-order spline. The arrows drawn above the curve represent the expected maxima at the appropriate product-ion energy corresponding to the product of various vibrational levels of N_2^+ resulting from collisions with the ^1S and ^5S states of N^+. It will be observed that the agreement between the expected positions of the $v=0,1,2,3$ states for the ^1S interaction with peaks from our data is very good. The agreement is also good for the $v=0,1,2$ levels which would be predicted from the ^5S state of N^+. Agreement with the ^5S state for values of $v=4,5$ is not nearly as good but appears to be satisfactory considering the signal-to-background ratio. Data for energies of 0.25 eV and larger are not sufficiently plentiful to allow an indexed plot to be made to aid in analysis.

It has been shown[24(a),(b)] that $N^+(^5S)$ as well as $N^+(^1S)$ is produced in quantity by electron impact on N_2. Because its lifetime is long it reaches the collisions point in our apparatus. The shape of the curve of Fig. 3, however, shows strong evidence of two spectral patterns, and an indexed plot of the positions of the maxima shown by the lines on Fig 3 shows a discontinuity at the

$v=0$ position of the ^1S state. Therefore the two spectral patterns belong to different systems.

The scattered ion intensity for most of the product-ion energies measured in the laboratory angle region between $-10°$ and $+10°$ is quite weak, broad, and structureless. However, we have obtained a number of energy scans at constant laboratory angle in that region. While the scattered ion intensity for $\theta_{lab}=0$ is very weak, it is possible to discern two peaks which are centered near 0.085 and 1.018 eV, respectively. The peak near 0.085 eV most likely corresponds to the reaction with ^1D nitrogen ions in which the product ions are produced in the $v=2$ vibrational state. A much harder collision can be observed centered at about product-ion energy 1.018 eV which corresponds to a large number of possible reaction with the ^1S state.

Table II shows the energy defect for eight possible reactions which need to be considered to explain the data of Figs. 2 and 3. The second column in Table II show the expected laboratory deflection angle θ_{lab} (for $\theta_{c.m.}=0$), the laboratory deflection which corresponds to each of the eight reactions. While $N^+(^3P)$ as well as $N^+(^1D)$ have previously been identified as the principal N^+ ions giving rise to the total charge-exchange cross section at least at low-impact energies, the data of Fig. 2 when extended into the position domain of θ_{lab} yields scattering of significantly less intensity than the peak scattering which appears at about $-17°$. Thus, reactions (1) and (5) do not contribute significantly to the total charge-exchange scattering cross section for the impact energies of this experiment. The same considerations apply to reactions (2) and (6) which, although contributing to the data shown are too low in intensity to be important in our analysis. Reactions (7) and (8) have been studied by Savage *et al.*[25] and Vance.[26] They have made measurements in our energy impact regime which show the presence of N_2^+ in an electron impact produced ion beam between 4% and 11% abundance. While N_2^+ is undoubtedly present in our ion beam, the predicted angle of deflection of N_2^+ formed from reaction seven is outside our domain of measurement or, as mentioned previously, is important only at high product-ion energies. We cannot rule out reaction (8) completely except to point out that the measured scattering intensity at $-27°$ is extremely low and that the production of $N_2^+(D\ ^2\Pi_g)$ has been determined to occur at very low intensity in electron impact excitation measurements[27] on N_2. Most reactions which involve the production of excited N_2^+ product-ion states are endothermic as has been seen in Table I. Therefore they will be seen, if at all, at values of θ_{lab} which are positive. Of the exothermic reactions involving excited N_2^+ states none corresponds to 3.006 eV, the defect giving size to scattering at $\theta_{lab}=-17°$.

For these reasons we assign reactions (3) and (4) as the major contributors to the observed differential charge-transfer scattering rather that the ^1D and ^3P states.[6,7] It is apparent that those states are not principal components of large-impact parameter, low center-of-mass angle charge-exchange scattering at about 100 V impact energy. Some measurements which we have made indicate that low-intensity scattering from ^3P and ^1D do in fact occur throughout the regime of available impact parameters, but it is certain that they do not contribute significantly in the range of $\theta_{c.m.}$ discussed in this paper.

The observation that the maximum charge-transfer scattering occurs at nearly zero center-of-mass angle has significant implications for the collisional charge-exchange process. Since the energy being transferred between the particles is about 3 eV, it is to be expected that a significant momentum transfer will occur between the colliding particles in the c.m. frame. Charge and vibrational energy-transfer measurements in the N_2^+ on N_2 system[27] have demonstrated that in that symmetric system, transfer of vibrational energy occurs at electronic state energy crossings which are nearly multiples of the vibrational frequencies of the isolated molecules. In addition, to account for the small center-of-mass angle of deflection which was observed, crossings were shown to occur during the approach phase of the collision so that the initial angle could be compensated during the exit phase by a nearly equal but oppositely directed deflection. Also, it was found that vibrational energy transfer occurs more efficiently for the exchanges of two or four quanta.

In contrast, for the N^+ on N_2 system the excitation of one–five quanta is seen to occur (Fig. 3) with approximately equal intensity with no "selection rule" for T-V or E-V transfer being apparent. Like N_2^+ on N_2, however, $N^+(^1S,^5S)$ on N_2 energy transfer occurs at almost zero c.m. deflection angle. This fact leads to the conclusion, as proposed in the case of N_2^+ on N_2, that the

TABLE II. Some charge-transfer reactions, energy defects, and predicted laboratory deflections for low center-of-mass angle scattering in the N^+-N_2 system.

Reaction	Energy defect (eV) for the product ion $N_2^+(X\ ^2\Sigma_g^+)$ in $v'=0$	Predicted θ_{lab} for $v=0$ and $\theta_{c.m.}=0°$
(1) $N_2+N^+(^3P)\rightarrow N_2^+(X)+N(^4S)$	−1.047	+5.3°
(2) $N_2+N^+(^1D)\rightarrow N_2^+(X)+N(^4S)$	0.852	−4.0°
(3) $N_2+N^+(^1S)\rightarrow N_2^+(X)+N(^4S)$	3.006	−16.2°
(4) $N_2+N^+(^5S)\rightarrow N_2^+(X)+N(^4S)$	4.706	−25.0°
(5) $N_2+N^+(^1D)\rightarrow N_2^+(X)+N(^2D)$	−1.532	+9.0°
(6) $N_2+N^+(^1S)\rightarrow N_2^+(X)+N(^2D)$	0.622	−2.2°
(7) $N_2+N_2^{2+}(X)\rightarrow N_2^+(X)+N_2^+(X)$	11.5	−49.0°
(8) $N_2+N_2^{2+}(X)\rightarrow N_2^+(D)$	5.0	−27.2

initial deflection produced by an attractive potential is compensated by a nearly equal repulsive potential after an electronic state crossing has occurred. A crossing which occurs during the approach phase is again to be preferred, since impact parameters near the potential minimum can be avoided and their consequent large contributions to the c.m. deflection angle can be greatly lessened.

The model just presented can reasonably be expected to produce a large array of vibrational product-ion states. Hence, the distribution of vibrational products shown in Fig. 3 is distinctly a nonFranck-Condon distribution. This is quite reasonable in view of the fact that the collision lifetime assuming a straight line trajectory is between 0.8 and 1.6×10^{-14} sec, a number comparable with the vibrational period of 1.5×10^{-14} sec. Moore *et al.*[28] and Ottinger *et al.*[29] have also found nonFranck-Condon product in distributions at low-collision energies in the N^+-N_2 system.

CONCLUSION

The data of this paper shows that $N^+(^1S)$ and $N^+(^5S)$ produced by 100 eV electron impact on N_2 is responsible for the major contribution to low center-of-mass charge-exchange scattering with N_2 in our impact energy range.

In order to produce the distribution of scattering intensities which we have observed, charge-exchange is most likely to occur during the approach phase of the collision and at large impact parameters. The effect of the collisional exchange of charge is to generate a nonFranck-Condon distribution of vibrational states in the product ion.

ACKNOWLEDGMENTS

The authors want to express their appreciation to R. E. Johnson for stimulating and helpful discussions.

[1]K. B. McAfee, Jr. and D. Edelson, Proceedings of the Sixth International Conference on Ionization Phenomena in Gases, Paris, 1963 (unpublished), p. 299; see also L. G. McKnight, K. B. McAfee, Jr., and P. P. Sipler, Phys. Rev. **164**, 62 (1967).

[2]E. Gustafsson and E. Lindholm, Ark. Fys. **13**, 219 (1960).

[3]R. F. Stebbings, B. R. Turner, and A. C. H. Smith, J. Chem. Phys. **38**, 2277 (1963).

[4]R. A. Moline, J. Appl. Phys. **42**, 2471 (1971).

[5]W. B. Maier and E. Murad, J. Chem. Phys. **55**, 2307 (1971).

[6]T. F. Moran and J. B. Wilcox, J. Chem. Phys. **70**, 1467 (1979).

[7](a) T. F. Moran and B. P. Mathur, Phys. Rev. A **21**, 1051 (1980); (b) P. A. Schulz, J. Chem. Phys. **83**, 5673 (1985).

[8]W. D. Watson, Ann. Rev. Astron. Astrophys. **16**, 585 (1978) and references therein.

[9]I. S. Bowen, Astrophys. J. **121**, 306 (1955).

[10]M. Oppenheimer, E. R. Constantinides, K. Kirby-Docken, C. A. Victor, A. Dalgarno, and J. H. Hoffman, J. Geophys. Res. **82**, 5485 (1977).

[11]D. G. Torr, M. R. Torr, W. B. Hansen, and J. H. Hoffman, Geophys. Res. Lett. **6**, 573 (1979).

[12]D. G. Torr and M. R. Torr, J. Atmos. Terr. Phys. **41**, 797 (1979).

[13]K. B. McAfee, Jr. and R. M. Lum, J. Geophys. Res. **81**, 4685 (1976).

[14]M. Saporoschenko, Phys. Rev. **11**, 1550 (1958).

[15]R. H. Varney, Phys. Rev. **93**, 1156 (1954).

[16]J. H. Moore Jr., Phys. Rev. A **8**, 2359 (1973).

[17]J. A. Rutherford and D. A. Vroom, J. Chem. Phys. **62**, 1460 (1975).

[18]K. B. McAfee, Jr., W. E. Falconer, R. S. Hozack, and D. J. McClure, Phys. Rev. A **21**, 827 (1980). See also Ref. 27.

[19]C. R. Szmanda, K. B. McAfee, Jr., and R. S. Hozack J. Phys. Chem. **86**, 1217 (1982).

[20]S. Bashkin and J. O. Stoner, Jr., *Atomic Energy Levels and Grotrian Diagrams* (Elsevier, New York, 1975), Vol. 1.

[21]J. L. Franklin, L. G. Dillard, H. M. Rosenstock, J. T. Herron, and K. Draxl, Natl. Bur. Stand. NSRDS Ref. Data Ser., Natl. Bur. Stand. (U.S.) Circ. No. 26 (U.S GPO, Washington, D.C., 1969).

[22]K. P. Huber and G. Herzberg, *Constants of Diatomic Molecules* (Van Nostrand Reinhold, New York, 1979).

[23]N. L. Schryer, in The Port Mathematical Subroutine Library, (1976), edited by P. Fox (Bell Telephone Laboratories, Murray Hill, New Jersey 07974).

[24](a) K. B. McAfee, Jr., C. R. Szmanda, and R. S. Hozack, J. Chem. Phys. **80**, 267 (1984); (b) R. Knight, Phys. Rev. Lett. **48**, 792 (1982).

[25]H. F. Savage and F. C. Witteborn, J. Chem. Phys. **48**, 1872 (1968).

[27]K. B. McAfee, Jr., C. R. Szmanda, and R. S. Hozack, J. Chem. Phys. **77**, 2399 (1982).

[28]J. H. Moore, Jr. and J. P. Doering, Phys. Rev. **177**, 218 (1969).

[29]C. Ottinger and J. Simonis, Chem. Phys. **28**, 97 (1978).